34th Annual International Conference of the IEEE EMBS
San Diego, California USA, 28 August - 1 September, 2012

Perturbationless Calibration of Pulse Transit Time to Blood Pressure

Mingwu Gao, *Student Member, IEEE* and Ramakrishna Mukkamala, *Member, IEEE*

***Abstract*—Pulse transit time (PTT) often shows strong correlation with blood pressure (BP) and may therefore represent a means for achieving continuous, non-invasive, and cuff-less BP monitoring. However, construction of the subject-specific curve needed to calibrate PTT to BP conventionally requires simultaneous measurements of PTT and BP during an experimental perturbation that varies BP over a significant range. We propose a technique for perturbationless calibration of PTT to BP. This technique constructs the calibration curve from central and peripheral BP waveforms by exploiting the natural pulsatile variation in the waveforms via a nonlinear tube-load model. We conducted initial testing of the technique in animals by applying it to the waveforms during a baseline period and then predicting mean BP during subsequent major hemodynamic interventions via PTT calibrated with the resulting curve. The bias in the mean BP error was 4.9 mmHg, while the precision in this error was 7.6 mmHg.**

I. Introduction

According to the well-known Bramwell-Hill equation, pulse transit time (PTT) declines with falling arterial compliance. Further, because collagen fibers are slack, arterial compliance falls with rising blood pressure (BP). As a result, PTT and BP are often inversely related. PTT therefore represents a potential means for achieving continuous, non-invasive, and cuff-less monitoring of BP. However, several problems must be overcome to achieve such ultra-convenient BP monitoring.

One problem pertains to the conventional foot-to-foot detection technique for estimating PTT from central and peripheral waveforms. This technique is prone to non-trivial error due to common artifact in the waveforms and wave reflection interference. As a result, there is often a great deal of scatter about the line of best fit between PTT and BP [1]. To mitigate this problem, we recently proposed to estimate PTT from the entire waveforms, rather than just their feet, after mathematically eliminating the reflected wave via a linear tube-load model or linear black-box model of the arteries [2, 3]. We showed that these linear techniques could indeed significantly reduce the scatter.

Another problem concerns the calibration of PTT to BP. To achieve this calibration, a subject-specific line or curve that relates PTT to BP is needed. A straightforward approach for constructing the curve is to measure both PTT and BP in a subject during an experimental perturbation that varies BP over a significant range. (BP could then be subsequently measured in that subject from only PTT by invoking the calibration curve.) However, the need for an experimental perturbation is a major drawback of this approach.

In this paper, we propose to construct the calibration curve relating PTT to BP by exploiting the natural pulsatile variation in BP. The basic idea is to incorporate a BP-dependent arterial compliance in the tube-load model and then estimate all parameters of this nonlinear model from central and peripheral BP waveforms. In this way, PTT may be ascertained for each and every value of BP during the cardiac cycle so as to establish the calibration curve. We describe proof-of-concept testing of this technique for "perturbationless" calibration of PTT to BP in animals during a broad array of major hemodynamic interventions. Our results show PTT-derived BP errors within FDA limits.

II. Methods

In this section, we begin by reviewing our linear tube-load model technique for robust estimation of the true PTT in the absence of wave reflection. Then, we introduce our nonlinear tube-load model technique for perturbationless calibration of PTT to BP. Finally, we describe our evaluation of the new technique.

A. Linear Tube-Load Model Technique for PTT Estimation

This technique estimates PTT from central and peripheral BP waveforms ($P_c(t)$ and $P_p(t)$) as shown in Fig. 1. First, a linear, uniform tube terminated by a lumped load is employed as a model of the relationship between the waveforms (see

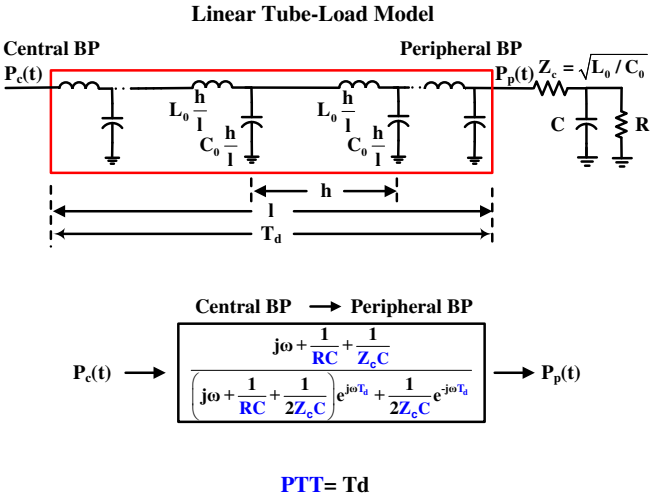

Fig. 1. Linear tube-load model technique.

Manuscript received May 31, 2012. This work was supported by a US National Science Foundation CAREER Grant [0643477] and by the Telemedicine and Advanced Technology Research Center (TATRC) at the U.S. Army Medical Research and Materiel Command (USAMRMC) through award W81XWH-10-2-0124.

M. Gao is with the Department of Electrical and Computer Engineering, Michigan State University, East Lansing, MI 48824 USA (Phone: 614-822-9399; fax: 517-353-1980; e-mail: gaomingw@msu.edu).

R. Mukkamala is with the Department of Electrical and Computer Engineering, Michigan State University, East Lansing, MI 48824 USA (e-mail: rama@egr.msu.edu).

Fig. 1). The tube represents the large artery path for wave to travel between the two measurement sites. The tube is frictionless, as large arteries offer little resistance to blood flow. Hence, the tube is equivalent to an ideal, lossless transmission line and has constant characteristic impedance ($Z_c = \sqrt{L_0/C_0}$), where L_0 and C_0 are large artery inertance and compliance while allowing waves to travel with constant PTT between the tube ends ($T_d = \sqrt{L_0 C_0}$) (Note that l is the length of the tube while h is the segmental length). The terminal load represents the small arteries distal to the peripheral artery measurement site. This load is characterized by peripheral resistance and compliance (R and C) while matching the tube impedance at infinite frequency. According to this model, the transfer function relating $P_c(t)$ to $P_p(t)$ is defined in terms of three unknown parameters, T_d, RC, and Z_cC (see Fig. 1). The three parameters are then estimated by finding the transfer function, which when applied to $P_c(t)$, best fits $P_p(t)$ in the least squares sense. This optimization is achieved by searching over a physiologic range of parameters. The PTT estimate is then given as T_d (see Fig. 1).

B. Nonlinear Tube-Load Model Technique for Perturbationless Calibration of PTT to BP

This technique constructs a subject-specific calibration curve relating PTT to BP from central and peripheral BP waveforms as shown in Fig. 2. More specifically, the technique builds upon the linear tube-load model technique by making the large artery segmental compliance dependent on BP according to the following exponential relationship from the literature [4]: $C_0 \frac{h}{l} \exp(-\alpha P)$, where α is an unknown parameter. Then, for a fixed BP, PTT and BP are related through the model parameters as follows:

$$\mathrm{PTT} = \sqrt{L_0 C_0 \exp(-\alpha P)}, \qquad (1)$$

Hence, by estimating the model parameters from the waveforms, this equation will constitute a subject-specific calibration curve. In this way, the calibration curve is formed based on the natural pulsatility in the waveforms without requiring an experimental perturbation.

However, since the model is nonlinear, the parameters

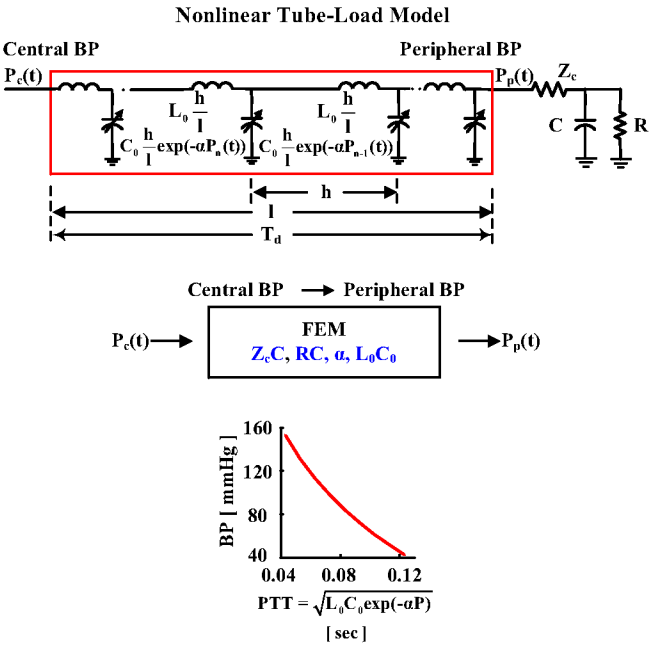

Fig. 2. Nonlinear tube-load model technique.

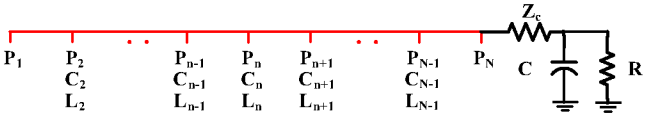

Fig. 3. Discretized nonlinear tube-load model for FEM calculation.

can no longer be estimated through a transfer function. A finite element method (FEM) is instead used as outlined in [5]. In particular, as shown in Fig. 3, the tube is discretized into N nodes. P_1 and P_N correspond to $P_c(t)$ and $P_p(t)$, while P_2 thru P_{N-1} represent the intermediate BPs. The compliance at each intermediate node is $C_n = C_0/(N-2)\exp(-\alpha P_n)$, and the inertance at the node is $L_n = L_0/(N-2)$. Then, after discretizing in time, $P_c(t)$ may be iteratively computed from $P_p(t)$ according to the following state-space equations:

$$\begin{bmatrix} P_1 \\ P_2 \\ P_3 \\ P_4 \\ P_5 \\ \vdots \\ P_{N-4} \\ P_{N-3} \\ P_{N-2} \\ P_{N-1} \end{bmatrix}^{k+1} = \begin{bmatrix} U^{k+1} \\ 0 \\ 0 \\ 0 \\ 0 \\ \vdots \\ 0 \\ 0 \\ 0 \\ 0 \end{bmatrix} + \begin{bmatrix} 0 & 0 & \ddots & 0 & 0 \\ \frac{(N-2)^2}{K_1}\Delta t^2 \exp(\alpha P_2^k) & 1-2\frac{(N-2)^2}{K_1}\Delta t^2 \exp(\alpha P_2^k) & \frac{(N-2)^2}{K_1}\Delta t^2 \exp(\alpha P_2^k) & \ddots & 0 \\ 0 & \frac{(N-2)^2}{K_1}\Delta t^2 \exp(\alpha P_3^k) & 1-2\frac{(N-2)^2}{K_1}\Delta t^2 \exp(\alpha P_3^k) & \frac{(N-2)^2}{K_1}\Delta t^2 \exp(\alpha P_3^k) & \ddots \\ \vdots & \ddots & \ddots & \ddots & \vdots \\ \ddots & \frac{(N-2)^2}{K_1}\Delta t^2 \exp(\alpha P_{N-2}^k) & 1-2\frac{(N-2)^2}{K_1}\Delta t^2 \exp(\alpha P_{N-2}^k) & \frac{(N-2)^2}{K_1}\Delta t^2 \exp(\alpha P_{N-2}^k) & 0 \\ 0 & \ddots & \frac{(N-2)^2}{K_1}\Delta t^2 \exp(\alpha P_{N-1}^k) & 1-2\frac{(N-2)^2}{K_1}\Delta t^2 \exp(\alpha P_{N-1}^k) & \frac{(N-2)^2}{K_1}\Delta t^2 \exp(\alpha P_{N-1}^k) \end{bmatrix}^2 \begin{bmatrix} P_1 \\ P_2 \\ P_3 \\ P_4 \\ P_5 \\ \vdots \\ P_{N-3} \\ P_{N-2} \\ P_{N-1} \\ P_N \end{bmatrix}^k \qquad (2)$$

$$P_N^{k+1} = \frac{\left(\frac{N-2}{\sqrt{K_1}K_2}\Delta t + \frac{N-2}{\sqrt{K_1}K_3}\Delta t + \frac{N-2}{\sqrt{K_1}}\right)\sum_{i=1}^{k}(P_{N-1}^i - P_N^i) - \frac{N-2}{\sqrt{K_1}}\sum_{i=1}^{k-1}(P_{N-1}^i - P_N^i) + \frac{1}{\Delta t}P_N^k}{\frac{1}{K_3}+\frac{1}{\Delta t}} \qquad (3)$$

where the superscript k denotes the time index and Δt is the time step. These equations have four unknown parameters, $K_1 = L_0C_0$, $K_2 = Z_cC$, $K_3 = RC$ and α. However, by first applying the linear tube-load model technique to the waveforms for analysis and determining mean BP, a single pair of PTT and BP results. Substituting this pair into Eq. (1) makes L_0C_0 completely determined by α. In this way, the number of unknown parameters are reduced to α, Z_cC and RC. These three parameters are estimated as follows. First, a physiologic range of parameters is selected. Then, each candidate set of parameters is substituted into Eqns. (2) and (3) to predict $P_p(t)$ from $P_c(t)$. Finally, the candidate set that

yields the minimum mean squared error between the predicted and measured $P_p(t)$ is chosen as the parameter estimates.

C. Technique Evaluation

The new technique was evaluated using previously collected data from five dogs. The data collection procedures were approved by the MSU All-University Committee on Animal Use and Care and are described in detail elsewhere [6]. Briefly, these data included invasive central (ascending aorta) and peripheral (femoral) BP waveforms from each dog during a baseline period and two to four interventions (amongst eight hemodynamic drugs, blood volume changes, and cardiac pacing) that varied mean BP over a wide range.

The new technique was applied to the BP waveforms only during the baseline period of each dog in order to construct a perturbationless calibration curve relating PTT to mean BP for that dog. Each calibration curve was then evaluated using the remaining intervention data of the corresponding dog as follows. First, the linear tube-load model technique was applied to the BP waveforms to estimate PTT for each 15-sec segment during the interventions. Then, mean BP was predicted from the resulting PTT and the calibration curve. Finally, the mean (bias) and standard deviation (precision) of the error between the predicted and measured mean BP was computed as quantitative evaluation metrics.

III. Results

Fig. 4 shows sample peripheral BP waveforms measured (blue) and predicted with the linear (black) and nonlinear (red) tube-load model techniques. As expected, the nonlinear tube-load model technique provided noticeably better waveform prediction than the linear tube-load model technique.

Fig. 5 shows a perturbationless calibration curve relating PTT to BP (red line) derived by the nonlinear tube-load model technique for one of the dogs. For comparison, the figure also includes pairs of PTT estimated by the linear tube-load model technique and measured mean BP (blue dots) during the interventions (i.e., data not seen by the nonlinear tube-load model technique) in that dog. The calibration curve corresponded reasonably well to these reference data pairs. Not surprisingly, the correspondence was best over the BP range seen by the nonlinear tube-load model technique (i.e., the mid-BP range).

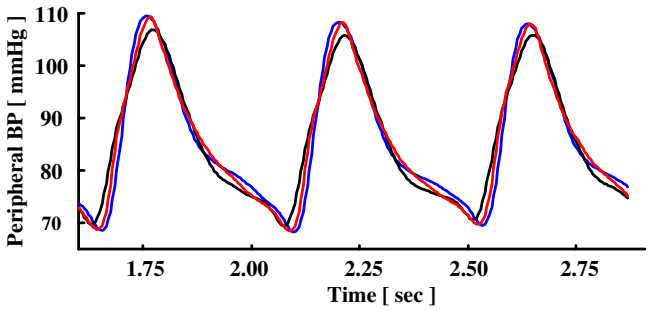

Fig. 4. Sample peripheral BP waveform measured (blue) and predicted by the linear (black) and nonlinear (red) tube-load model techniques.

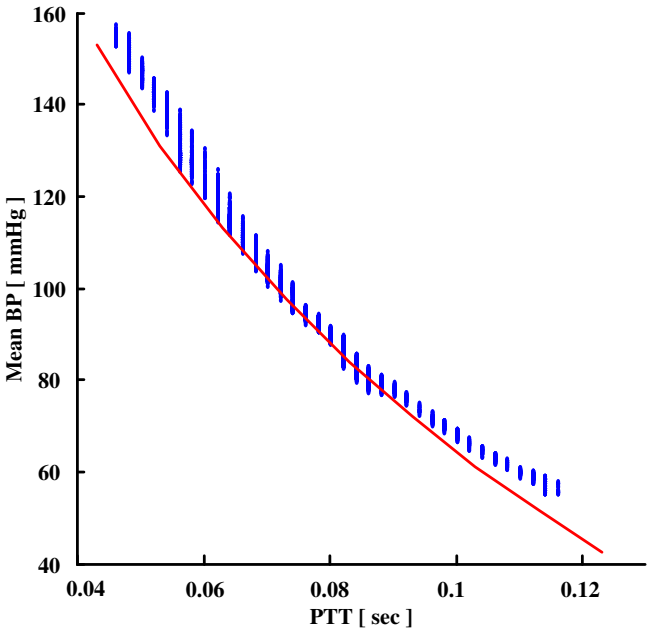

Fig. 5. Sample perturbationless calibration curve constructed by the nonlinear tube-load model technique for one of the dogs (red line) along with reference values (blue dots).

TABLE I: Quantitative Results of the Nonlinear Tube-Load Model Technique Per Dog [mmHg]

Dog	Mean BP Range	μ	σ
1	57-167	6.83	9.40
2	59-111	5.36	5.00
3	55-158	2.93	3.39
4	26-133	1.44	9.31
5	45-166	8.10	10.75
Average	48-147	4.93	7.57

Table I shows the quantitative results per dog of the perturbationless calibration of PTT to mean BP by the nonlinear tube-load model technique. Mean BP varied, on average, from 48 to 147 mmHg. The group average bias (μ) in the mean BP error was 4.9 mmHg, while the group average of the precision (σ) in this error was 7.6 mmHg.

IV. Discussion

In summary, PTT represents a potential vehicle for achieving continuous, non-invasive, and cuff-less BP monitoring. However, construction of the subject-specific curve needed to calibrate PTT to BP conventionally requires simultaneous measurement of PTT and BP during an experimental perturbation that varies BP over an appreciable range. Here, we proposed a nonlinear tube-load model technique that is able to construct the calibration curve from central and peripheral BP waveforms without the need for an experimental perturbation by exploiting the natural pulsatile variation in the waveforms. We tested the technique in animals. Our results showed mean BP errors that are within the FDA limits of 5 mmHg bias and 8 mmHg precision.

In this proof-of-concept study, we applied and tested the nonlinear tube-load model technique using invasive BP waveforms. In practice, the technique could be applied to

non-invasive carotid (central) and femoral (peripheral) BP waveforms obtained via a hand-held applanation tonometer to establish the perturbationless calibration curve. Thereafter, PTT could be measured from carotid and femoral photoplethysmography (i.e., pulse oximetry) waveforms and then calibrated with the curve to achieve continuous, non-invasive, and cuff-less monitoring of mean BP. Note that several other possibilities for practical implementation could also be envisaged.

The calibration curve could change in a subject with vasomotor tone. However, the aorta is relatively sparse in smooth muscle [7]. So, by measuring PTT through the aorta (as done here), this confounding mechanism can be mitigated. The calibration curve could also change due to aging and disease. Fortunately, these confounding processes are often slow. As a result, the calibration curve could be updated every few months or possibly even years.

Finally, we did not address the problem of measuring systolic and diastolic BP via PTT here. We hope to tackle this challenging problem in the future.

REFERENCES

[1] JD. Pruett, "Measurement of pulse-wave velocity using a beat-sampling technique" Ann Biomed Eng 16: 341-347, 1988.

[2] G. Zhang, "Robust, Beat-to-Beat Estimation of the True Pulse Transit Time from Central and Peripheral Blood Pressure or Flow Waveforms Using an Arterial Tube-Load Model" Proceeding of 33rd Annual International Conference of the IEEE EMBS 2011, pp. 4291-4294.

[3] D. Xu, "Improved pulse transit time extimation by system identification analysis of proximal and distal arterial waveforms" Am J Physiol Heart Circ Physiol 301: H1389-H1395, 2011.

[4] D.J. Hughes, "Measurements of Young's modulus of elasticity of the canine aorta with ultrasound. Ultrasound Imaging 1(4), 356-67 1979.

[5] S. Lee, "Lossy Transmission Line Transient Analysis by the Finite Element Method." Magnetics, IEEE Transactions on, Mar 1993, Vol 29, Issue 2, pp: 1730-1732.

[6] G. Swamy, "An adaptive transfer function for deriving the aortic pressure waveform from a peripheral artery pressure waveform," Am J Physiol-Hear C, vol. 297, pp. H1956-H1963, Nov 2009.

[7] AC. Burton, "Relation of structure to function of the tissues of the wall of blood vessels," Physiol Rev 34: 619-642, 1954.